

# Mix Design of Ambient Cured Geopolymer Concrete with Fly Ash, GGBFS, and Borax

Eklisia Hanani, Iman Satyarno\*, and Djoko Sulistyono

Department of Civil and Environmental Engineering, Universitas Gadjah Mada, Yogyakarta 55281, Indonesia

Keywords:  
Geopolymer  
Fly ash  
GGBFS  
Borax additive  
Ambient cured

## ABSTRACT

Geopolymer cement, using fly ash (FA), presents a viable alternative to Portland cement. However, FA-based geopolymers often lack reactivity and strength, necessitating combination with calcium-rich materials like ground granulated blast furnace slag (GGBFS). However, GGBFS could accelerate setting and decrease workability, requiring a retarder. Borax is recognized for its retarding properties in FA-based geopolymers, but its impact in FA-GGBFS systems remains understudied. This study evaluated the influence of varying proportions of FA and GGBFS with the addition of borax, on the setting time, workability, and mechanical strength of the geopolymer paste, mortar, and concrete under ambient curing conditions. Setting time test was conducted for the geopolymer paste, flow table test for workability assessment of mortar, and compressive strength testing at 1, 7, and 28 days for the mechanical strength of paste and concrete. Various FA:GGBFS ratios (100:0, 70:30, 50:50, and 0:100) were examined. Alkali activator consists of NaOH and Na<sub>2</sub>SO<sub>3</sub> with Na<sub>2</sub>SO<sub>3</sub>/NaOH ratio (R) of 1.5 and alkali to precursors ratio (A) of 0.45 was used. Borax was added at a constant 3% by weight of the precursors. Both the volume ratios of paste to fine aggregate voids ( $R_m$ ) and mortar to coarse aggregate voids ( $R_b$ ) were set to 1.5. Borax increased initial setting time by 7-33 minutes for FA-GGBFS geopolymer. GGBFS replacement decreased the workability of mortar, with flow index ranging from 83-158%. Increasing GGBFS content significantly improved compressive strength in both paste and concrete samples. Notably, 100% GGBFS replacement yielded the highest concrete strength at 74.86 MPa after 28 days. However, the optimal balance of properties was achieved with a 50% GGBFS replacement, resulting in satisfactory strengths of 100.29 MPa for paste and 69.08 MPa for concrete, along with a 40-minute initial setting time and a flow index of 138%. These findings surpass prior studies on similar geopolymers.



This is an open access article under the [CC-BY](https://creativecommons.org/licenses/by/4.0/) license.

## 1. Introduction

High energy intensity production processes associated with OPC make the global cement industry one of the most significant energy consumers and CO<sub>2</sub> emitters [1], [2]. As the global construction industry seeks innovative and environmentally conscious solutions, alternatives to traditional Portland cement-based materials are being explored [3]. The prevalent adoption of alternative materials as a replacement for cement has significantly reduced the carbon footprints of cement, leading to the development of terms like "green concrete" or geopolymer concrete (GPC). Geopolymer concrete presents numerous benefits compared to conventional Portland cement concrete, including up to an 80% reduction in carbon emissions, high strength, durability, and good resistance to harsh environments [4], [5], [6], [7], [8].

Geopolymer concrete is fabricated by activating the precursor material using an alkali activator [9]. Fly ash (FA) is classified as Class C or Class F based on ASTM C618-22 criteria, with both classes requiring a minimum total weight percentage of SiO<sub>2</sub> + Al<sub>2</sub>O<sub>3</sub> + Fe<sub>2</sub>O<sub>3</sub> of 50%, while the CaO content should exceed 18% for Class C and be limited to a maximum of 18% for Class F. In contrast to Class C fly ash, which displays considerable reactivity, Class F fly ash often presents low reactivity and gradual strength development. To expedite the dissolution of Si and Al in Class F fly ash-based geopolymers, heat curing or the inclusion of mineral additives with elevated calcium content may be necessary [10]. To mitigate the limitations of a single precursor geopolymer, a common approach involves blending multiple precursors, utilizing their combined strengths to enhance properties such as durability and mechanical properties [11], [12]. One of the frequently

\*Corresponding author.

E-mail: [imansatyarno@ugm.ac.id](mailto:imansatyarno@ugm.ac.id)

<http://dx.doi.org/10.21831/inersia.v20i2.74464>

Received 10<sup>th</sup> June 2024; Revised 31<sup>st</sup> December 2024; Accepted 31<sup>st</sup> December 2024

Available online 31<sup>st</sup> December 2024

explored combinations is geopolymer formulations based on a mixture of fly ash and GGBFS, which has garnered attention from numerous researchers in the field [13], [14], [15]. The results of these investigations revealed that the compressive strength of class F FA-based geopolymer concrete improves with increasing GGBFS dosage.

Previous study highlighted the potential of class F FA-GGBFS geopolymer in producing concrete with low to moderate strength, eliminating the necessity for heat curing [16]. Another study investigated the reactivity and microstructure of FA-GGBFS based mixture [17]. The findings revealed that replacing class F FA with GGBFS up to 30% increased compressive strength under ambient curing conditions, with a maximum strength of 45 MPa observed in GPC mixtures containing 70% FA and 30% GGBFS. The maximum strength achieved with GGBFS surpassed that of FA alone due to unreactive FA under ambient curing conditions. Similar results were reported, demonstrating that GGBFS played a crucial role in enhancing strength, with a maximum of 56.43 MPa in 100% GGBFS mixture, reducing the porosity, denser matrix, albeit with a decrease in setting time [18].

Based on prior research, the incorporation of fly ash and GGBFS mixture has been identified to enhance strength, particularly with an escalation in GGBFS content due to the high CaO content and reactivity. However, this intensified use of GGBFS is associated with shorter setting times and decreased workability. Another viable option would be to incorporate retarders and rheology-modifiers, which are commonly used in OPC concretes. However, these admixtures often exhibit inefficiency or ineffectiveness in geopolymer systems, with their efficacy largely contingent upon factors such as the alkaline nature of the activators and the mixes composition [19], [20]. Insights from a study suggested that the inclusion of borax can extend setting time which acts as a retarder [21]. However, this study was conducted solely on fly ash as the precursor, and the high dosage of borax resulted in a notable reduction in compressive strength.

This paper investigates the optimal mix design of ambient cured FA-GGBFS-based geopolymer concrete with low dosage borax as an admixture, assessing its impact on setting time, workability, and compressive strength of geopolymer paste, mortar, and concrete. The outcomes of this investigation hold potential for advancing geopolymer concrete technology by leveraging the combination of fly ash, GGBFS, and borax to enhance compressive strength, achieve favorable workability, and ensure adequate setting time.

## 2. Methods

### 2.1 Materials

#### 2.1.1 Precursors

Precursors, in the context of this study, were the raw materials essential for producing geopolymer materials. The precursors utilized here include FA and GGBFS. The locally sourced FA was derived from the Paiton power plant in East Java, Indonesia, while the GGBFS was obtained from PT Krakatau Semen Indonesia. The X-ray fluorescence (XRF) analysis, as detailed in [Error! Reference source not found.](#), provided a breakdown of the oxide composition of FA and GGBFS.

**Table 1.** XRF analysis of FA and GGBFS (% mass)

Component	Fly Ash	GGBFS
Al <sub>2</sub> O <sub>3</sub>	23.8	15.45
SiO <sub>2</sub>	48.7	36.52
Fe <sub>2</sub> O <sub>3</sub>	11.0	0.98
CaO	12.7	44.38
SO <sub>3</sub>	1.34	0.07
K <sub>2</sub> O	0.97	0.33

FA could be sorted into Class C and F based on ASTM C618-22 criteria, where the distinction relied on the CaO content. Class F fly ash, characterized by a maximum CaO content of 18%, displayed pozzolanic properties, whereas class C fly ash, with a higher CaO content (>18%), exhibited both pozzolanic and cementitious properties. The required minimum sum of SiO<sub>2</sub>, Fe<sub>2</sub>O<sub>3</sub>, CaO, and Al<sub>2</sub>O<sub>3</sub> for both classes was 50%.

Following the current standard (ASTM C618-22), the fly ash utilized was categorized as Class F due to its CaO content being below 18% (specifically, CaO 12.7%) and meeting the minimum sum of SiO<sub>2</sub>, Fe<sub>2</sub>O<sub>3</sub>, CaO, and Al<sub>2</sub>O<sub>3</sub>, which amounted to 83.5%. It is noteworthy that despite being categorized as class F in this study, the fly ash demonstrates a short setting time and could be cured under ambient temperature, characteristic typically associated with class C fly ash.

The reactivity of fly ash was associated with its glassy constituents. The typical glass composition of high-calcium fly ash is such that anorthite and gehlenite are the first minerals to form when it cools from a molten state. In contrast, low-calcium fly ash tends to form mullite as its main crystalline phase under similar conditions. As depicted in **Figure 1**, the fly ash utilized in this study fell within the anorthite range, which is characteristic of high-calcium fly ash (Class C). This likely accounts for the observed high reactivity of the fly ash.

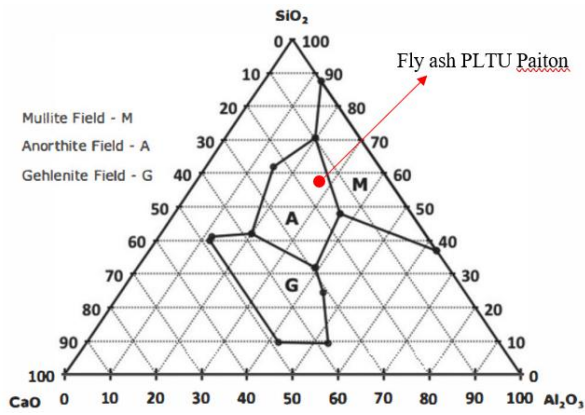


Figure 1 Ternary diagram of fly ash from Paiton power plant

1.1.2 Alkali activator

To activate the precursors, a combined alkali activator of sodium hydroxide (NaOH), sodium silicate (Na<sub>2</sub>SiO<sub>3</sub>), and borax pentahydrate was utilized. NaOH pellets with 98% purity were obtained from PT AKR Corporindo Tbk. Na<sub>2</sub>SiO<sub>3</sub> solution was obtained from PT Sinar Sakti Kimia, with a density of 1.68. Borax pentahydrate ETIMADEN with 99.9% purity was obtained from Intiprimacool, an online e-commerce store.

The NaOH solution was made by dissolving NaOH flakes (98% purity) in distilled water to achieve a 10 M concentration. Borax is introduced into the process after creating the NaOH solution while the solution is hot, facilitating borax dissolution and homogenization. The weight of borax is calculated as a constant percentage of 3% to the weight of precursors in the mixture. The prepared solution was then brought down to room temperature for 24 hours before use. The solution was then combined with the Na<sub>2</sub>SiO<sub>3</sub> solution in a ratio of *R* (Na<sub>2</sub>SiO<sub>3</sub>/NaOH) = 1.5, and cooled for at least an hour before ready to be used for mixing. The alkali to precursor ratio (A) employed in this study remained constant at 0.45, thereby ensuring optimal workability and sufficient setting time.

The variables in this research are based on a review of previous studies, including research conducted previously which investigated various combinations of alkali activators and found that the combination of NaOH and Na<sub>2</sub>SiO<sub>3</sub> produced superior concrete performance [18]. Moreover, previous research highlighted that utilizing a high alkali concentration of NaOH (10M-

14M) is conducive to achieving high-strength geopolymer concrete and enhancing precursor reactivity [22]. Additionally, investigation of the impact of alkali to precursor ratio on setting time in a mixture containing FA and GGBFS, affirming that a lower ratio (0.35) notably shortened the setting time and decreased the workability [23]. Similar observation reported that a lower alkali to precursor ratio (0.28-0.32) increased strength while compromising the workability of the mixture [24]. The choice of a low borax percentage (3%) in this study aims to minimize production costs and prevent a significant reduction in compressive strength, as compared to previous study where a high dosage of borax resulted in a significant decrease in compressive strength [21]. Lastly, the selection of a ratio of *R* (*SS/SH*) = 1.5 is motivated by the need to achieve a workable mixture where it has been observed that a high *R* ratio (2-2.5) can significantly reduce the workability of the mixture [24]. A lower ratio of *R* (1.5) is also to prevent an excess of silicate content in the mixture, which could hinder the formation of the geopolymeric structure and aggravate water evaporation issues [18], [25], [26].

1.1.3 Aggregates

The aggregates properties and standards utilized to test its properties are outlined in Table 2 The source of fine aggregates was from Kali Progo, Yogyakarta categorized as zone 2 can be seen in Figure 2, while the coarse aggregate employed was local crushed stone sourced from Clereng, Yogyakarta, with a maximum diameter of 10 mm. Both fine and coarse aggregates were utilized in saturated surface dry (SSD) conditions, adhering to ASTM C136 specifications.

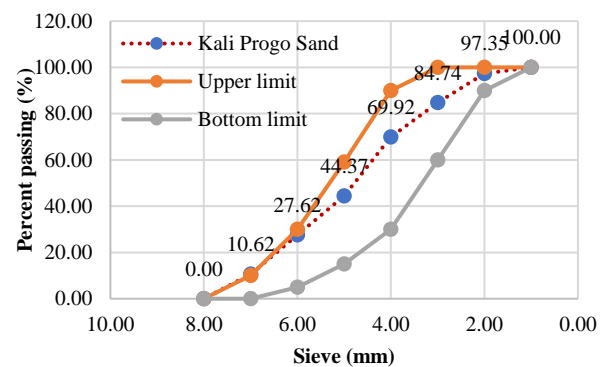


Figure 2. Sand grading zone II

Table 2. Aggregates characteristics

Characteristic	Fine aggregate	Coarse aggregate	Standards
Gradation	Zone 2	-	
Fineness modulus	2.65	6.86	SNI 03-1968-1990
Compacted unit weight	1601.08 kg/m <sup>3</sup>	1469.67 kg/m <sup>3</sup>	
loose unit weight	1298.89 kg/m <sup>3</sup>	1294.29 kg/m <sup>3</sup>	SNI 03-4804-1998
Specific gravity (dry)	2.583	2.540	SNI 1969:2008 (coarse agg.)
Specific gravity (SSD)	2.679	2.619	SNI 1970:2008 (fine agg.)
Organic matter content	satisfied the standard	-	SNI 2816:2014
Mud content	3.38 (<5%)	-	SNI 03-4142-1996
Abrasion	-	20.66% < 27%*	SNI 2417:2008;
		*for f'c > 20 MPa	SII 0052-80/SK-SNI. S-0401989

**1.1.4 Design mix proportion**

The composition was formulated using the absolute volume method, given the absence of an established standard regulating the formulation of geopolymer concrete at the time. This method aligned with the approach outlined in the previous research [27], utilizing the absolute volume method for geopolymer paste as defined in Equation (1).

$$\frac{W_{fa}}{G_{s_{fa}} \gamma_w} + \frac{W_{ggbfs}}{G_{s_{ggbfs}} \gamma_w} + \frac{W_{ss}}{G_{s_{ss}} \gamma_w} + \frac{W_{sh}}{G_{s_{sh}} \gamma_w} = 1 \text{ m}^3 \quad (1)$$

Where:  $W_{fa}$  = weight of fly ash,  $G_{s_{fa}}$  = specific gravity of fly ash,  $W_{ggbfs}$  = weight of GGBFS,  $G_{s_{ggbfs}}$  = specific gravity of GGBFS,  $W_{ss}$  = weight of sodium silicate,  $G_{s_{ss}}$  = specific gravity of sodium silicate,  $W_{sh}$  = weight of sodium hydroxide,  $G_{s_{sh}}$  = specific gravity of sodium hydroxide, and  $\gamma_w$  = density of water (1000 kg/m<sup>3</sup>).

The ratio parameters  $A$  (alkali to precursor ratio),  $R$  (alkali activator ratio), and  $X$  (GGBFS to FA ratio) can be determined by Equations (2), (3), and (4).

$$A = \frac{W_{ss} + W_{sh}}{W_{fa} + W_{ggbfs}} \quad (2)$$

$$R = \frac{W_{ss}}{W_{sh}} \quad (3)$$

$$X = \frac{\text{GGBFS (\%)}}{\text{FA (\%)}} \quad (4)$$

The weight of sodium hydroxide ( $W_{sh}$ ) and sodium silicate ( $W_{ss}$ ) can be calculated by correlating the ratio of  $A$ ,  $R$ , and  $X$ , as follows:

$$W_{ss} + W_{sh} = A(W_{fa} + W_{ggbfs}) \quad (5)$$

$$RW_{sh} + W_{sh} = A(W_{fa} + XW_{fa}) \quad (6)$$

$$(1 + R)W_{sh} = A(1 + X)W_{fa} \quad (7)$$

$$W_{sh} = \frac{A(1+X)}{(1+R)} W_{fa} \quad (8)$$

$$W_{ss} = \frac{AR(1+X)}{(1+R)} W_{fa} \quad (9)$$

This study utilized borax as an additive, the weight of borax could be calculated using equation (10).

$$W_{br} = B(W_{fa} + W_{ggbfs}) \quad (10)$$

Where:  $W_{br}$  = weight of borax,  $B$  = percentage of borax added.

Equation (1) was then simplified using the ratio parameters  $A$  (alkali to precursor ratio),  $R$  (alkali activator ratio), and  $X$  (GGBFS to FA ratio), therefore the design equation for FA-GGBFS geopolymer paste utilizing the absolute volume method is obtained as follows:

$$\frac{W_{fa}}{G_{s_{fa}} \gamma_w} + \frac{(X)W_{fa}}{G_{s_{ggbfs}} \gamma_w} + \frac{AR(1+X)W_{fa}}{G_{s_{ss}} \gamma_w} + \frac{A(1+X)W_{fa}}{G_{s_{sh}} \gamma_w} = 1 \text{ m}^3 \quad (11)$$

Based on Equation (11), the mixture proportions of geopolymer paste are detailed in

**Table 3.**

The composition of the mortar mix was established according to the composition of the paste mix. By modifying Equation (11), the composition of the mortar mix could be calculated by Equation (12). The composition of geopolymer mortar mix with optimal rheological and mechanical properties was obtained by assuming that the volume of fine aggregate voids was exactly filled by the volume of paste. The formulation of geopolymer mortar mix was closely associated with the parameter  $R_m$ , representing the ratio of the absolute volume of paste ( $V_p$ ) to the volume of voids between fine aggregate particles ( $V_{r_{agh}}$ ).

$$\frac{W_{fa}}{G_{s_{fa}} \gamma_w} + \frac{(X)W_{fa}}{G_{s_{ggbfs}} \gamma_w} + \frac{AR(1+X)W_{fa}}{G_{s_{ss}} \gamma_w} + \frac{A(1+X)W_{fa}}{G_{s_{sh}} \gamma_w} = V_{r_{agh}} R_m \quad (12)$$

The absolute volume ratio of geopolymer paste to the volume of fine aggregate voids ( $R_m$ ) can be calculated using Equation (13).

$$R_m = \frac{V_p}{V_{r_{agh}}} \tag{13}$$

The volume of voids between fine aggregate particles ( $V_{r_{agh}}$ ) in 1 m<sup>3</sup> can be calculated by Equation (14).

$$V_{r_{agh}} = 1 - \frac{B_{s_{agh}}}{G_{s_{agh}}} \gamma_w \tag{14}$$

Based on Equation (12), the mixture proportion of geopolymer mortar can be seen in **Error! Reference source not found.**. To be noted, the variable  $R_m$  is predetermined by 1.5 based on the optimum ratio of a previous study done by [22].

The composition of the geopolymer concrete mix was established by modifying the compositions of the geopolymer paste and mortar mix. Therefore, the design equation for geopolymer concrete using the absolute volume method is derived as Equation (15). To achieve the optimal rheological and mechanical properties of the geopolymer concrete, it was assumed that the volume of fine aggregate voids ( $V_{r_{agh}}$ ) was entirely filled by the paste volume ( $V_p$ ), while the volume of coarse aggregate voids ( $V_{r_{agk}}$ ) was filled by the mortar volume ( $V_m$ ).

$$\frac{W_{fa}}{G_{s_{fa}} \gamma_w} + \frac{(X)W_{fa}}{G_{s_{ggbfs}} \gamma_w} + \frac{AR(1+X)W_{fa}}{G_{s_{ss}} \gamma_w} + \frac{A(1+X)W_{fa}}{G_{s_{sh}} \gamma_w} = V_{r_{agh}} R_m V_{r_{agk}} R_b \tag{15}$$

The volume of voids between coarse aggregate particles ( $V_{r_{agk}}$ ) in 1 m<sup>3</sup> could be calculated by Equations (16).

$$V_{r_{agk}} = 1 - \frac{B_{s_{agk}}}{G_{s_{agk}}} \gamma_w \tag{16}$$

The absolute volume ratio of geopolymer mortar to the volume of fine aggregate voids ( $R_b$ ) can be calculated using Equation (17).

$$R_b = \frac{V_m}{V_{r_{agk}}} \tag{17}$$

To be noted, the variables  $R_m$  and  $R_b$  are predetermined as 1.5, based on the previous study by [22] which showed optimum mechanical properties.

Based on Equation (15), the mixture proportion of geopolymer concrete is shown in **Error! Reference source not found.**

**Table 3.** Geopolymer paste mixture proportion

Mix ID	Mix label	Paste mixture quantity (kg/m <sup>3</sup> )					A	M	R
		FA	GGBFS	SS	SH	Borax			
PF100G0	PF100G0M10A45B3R15	1535.4	0.0	414.5	276.4	46.1	0.45	10	1.5
PF70G30	PF70G30M10A45B3R15	1092.0	468.0	421.2	280.8	46.8	0.45	10	1.5
PF50G50	PF50G50M10A45B3R15	788.4	788.4	425.7	283.8	47.3	0.45	10	1.5
PF0G100	PF0G100M10A45B3R15	0.0	1620.6	437.6	291.7	48.6	0.45	10	1.5

*Label:* FA = fly ash, GGBFS = ground granulated blast furnace slag, SS = sodium silicate, SH = sodium hydroxide, A ratio = Alkali/precursor ratio, M = NaOH molarity, R = Na<sub>2</sub>SO<sub>3</sub> to NaOH ratio.

**Table 4.** Geopolymer mortar mixture proportion

Mix ID	Mix label	Mortar mixture quantity (kg/m <sup>3</sup> )									
		FA	GGBFS	SS	SH	Borax	Sand	A	M	R	V <sub>r<sub>agh</sub></sub>
MF100G0	MF100G0M10A45B3R15Rm15	926.6	0.0	250.2	166.8	27.8	1062.2	0.45	10	1.5	0.40
MF70G30	MF70G30M10A45B3R15Rm15	659.0	282.4	254.2	169.5	28.2	1062.2	0.45	10	1.5	0.40
MF50G50	MF50G50M10A45B3R15Rm15	475.8	475.8	256.9	171.3	28.5	1062.2	0.45	10	1.5	0.40
MF0G100	MF0G100M10A45B3R15Rm15	0.0	978.0	264.1	176.0	29.3	1062.2	0.45	10	1.5	0.40

**Table 5.** Geopolymer concrete mixture proportion

Mix ID	Mix label	Concrete mixture quantity (kg/m <sup>3</sup> )										V <sub>r<sub>ag<sub>h</sub></sub></sub>	V <sub>r<sub>ag<sub>k</sub></sub></sub>
		FA	GGBFS	SS	SH	Borax	Sand	CA	A	M	R		
CF100G0	CF100G0M10A45B3R15Rb Rm15	609.9	0.0	164.7	109.8	18.3	699.2	895.1	0.4	10	1.	0.40	0.44
CF70G30	CF70G30M10A45B3R15Rb Rm15	433.8	185.9	167.3	111.5	18.6	699.2	895.1	0.4	10	1.	0.40	0.44
CF50G50	CF50G50M10A45B3R15Rb Rm15	313.2	313.2	169.1	112.7	18.8	699.2	895.1	0.4	10	1.	0.40	0.44
CF0G100	CF0G100M10A45B3R15Rb Rm15	0.0	643.7	173.8	115.9	19.3	699.2	895.1	0.4	10	1.	0.40	0.44

### 1.1.5 Mixing, curing and testing

Paste samples for setting time and compressive strength tests were prepared using a Hobart N50 mixer. Initially, precursors consist of FA and GGBFS, were added to the mixer and dry-mixed until both materials were combined. Subsequently, the alkali activator was added and mixed for 3 minutes to produce a uniform paste. The setting time (initial and final) of the fresh geopolymer paste were assessed using a Vicat needle apparatus, following the ASTM C191 standard procedure with measurements recorded at 1-minute intervals. Compressive strength tests for the geopolymer paste using 50 mm cube molds were carried out at 1, 7, and 28 days of age to evaluate the compressive strength, tested in accordance to ASTM C109.

The geopolymer mortar mixing process started with making geopolymer paste, by mixing the precursors (FA and GGBFS) and alkali activator until uniform. Then, fine aggregate was added, and the mixture underwent further mixing for 3-5 minutes until all materials were thoroughly combined. The mortar samples underwent flow table testing following ASTM C230 and ASTM C1437 standards. This test was conducted directly following the mixing process to assess the flowability of the fresh geopolymer mortar. The flow test measured the flow diameter, which indicates the spread behavior of the paste after a specified number of drops (25 drops), across various mixture proportions.

Concrete samples for compressive strength test were mixed using the Creteangle Multi Flow Mixer (0.2 m<sup>3</sup> capacity). The method involved creating the paste mixture by combining precursors (fly ash and GGBFS) and alkali activator, followed by the addition of both fine and coarse aggregates. The mixture was then mixed for 7-10 minutes until uniform. The prepared concrete mixture was cast into 100 x 200 mm cylindrical molds in three layers with standard compaction according to SNI 4810:2013 or ASTM C31. For concrete samples containing 100% GGBFS (CF0G100), compaction was achieved using a vibrator due to its stiff consistency. The moulds were wrapped with plastic film immediately after casting to avoid water evaporation and left overnight before demolding the next day. After demolding, the specimens were fully wrapped in a plastic sheet and allowed to cure under ambient laboratory conditions. Compressive strength tests were carried out at 1, 7, and 28 days.

## 3. Results and Discussion

### 1.2 Setting time of geopolymer paste

The initial setting time in geopolymer refers to the duration it takes for the geopolymer paste to begin solidifying after mixing and the needle penetrates to a depth of 25 mm. Final setting time refers to the duration until the needle cannot

penetrate. To examine the impact of incorporating borax into the mixture, a comparison was made with the same mix design but without the addition of borax, focusing on initial and final setting time can be seen in **Figure 3**.

Based on the test results, 3% borax was able to extend the setting time by 7-33 minutes compared to the mixture with 0% borax, with the longest setting time was found in 30% GGBFS substitution mix (PF70G30) with the initial and final setting of 44 and 57 minutes. It is worth mentioning that in the specimen with 100% GGBFS and 0% borax there was a flash setting during mixing so there was no recording of setting time. As highlighted by [28], anhydrous borax introduces [BO<sub>4</sub>] tetrahedra into the mixture. While the bonding of [BO<sub>4</sub>] with [SiO<sub>4</sub>] is easy, its interaction with [AlO<sub>4</sub>] or even within [BO<sub>4</sub>] tetrahedra themselves presents challenges. This intricate process contributes to the retarding effect observed with anhydrous borax. This discovery aligns with findings from previous studies, which also indicate that the addition of borax to geopolymer concrete mixtures tends to prolong the setting time [21], [23], [28], [29], [30], [31], [32], [33].

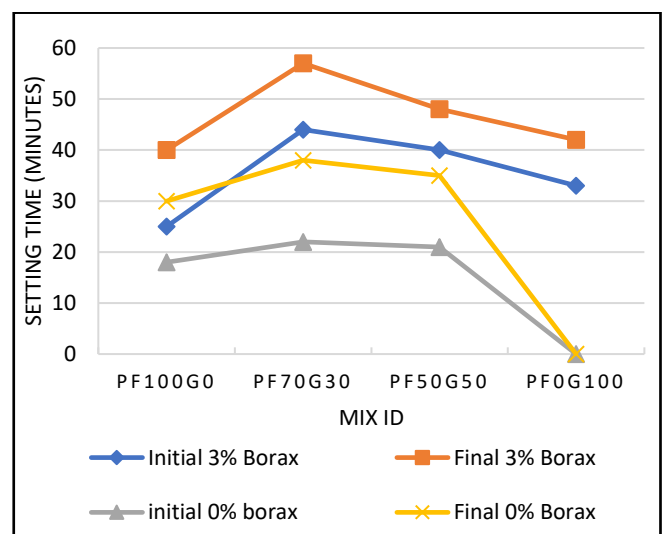
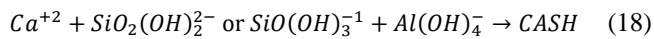


**Figure 3.** Setting time of geopolymer paste with 0% and 3% borax.

In the case of 30% GGBFS replacement (PF70G30), the initial setting time was prolonged by 19 minutes compared to the mixture containing only FA (PF100G0), as depicted in **Figure 3**. 100% FA mixtures exhibited the shortest setting time and high reactivity compared to others. This finding contrasts with previous studies where increasing GGBFS substitution accelerated setting time in FA-GGBFS based geopolymer concrete, where high CaO content in GGBFS typically enhances polymerization by forming Ca-Al-Si gel and speeding up the setting time [16], [18], [34], [35]. However, the difference in the results of this study can be caused by the FA content itself. FA from PLTU Paiton used

in this study was characterized by high alumina and silica contents. The relationship between Si, Al, and Ca content and the speed of hardening time has been investigated in several studies. As described by [36], the process and hardening time of FA-based geopolymer is controlled by the initial formation of CASH, where Al and Si concentrations are important factors in this process. The CASH precipitation reaction is as follows:



CASH is stable in high pH environments (>13), having a dominant role in setting time. At high alkaline pH, there is rapid dissolution of  $Al_2O_3$  and  $SiO_2$  with high reactivity resulting in high concentrations of silica and alumina in the initial phase. These compounds then react with  $Ca^{2+}$  ions to form the CASH phase which leads to shorter hardening times. Previous study also stated that the geopolymerization process is controlled by the exothermic peak that occurs in the geopolymer chemical reaction, where this exothermic peak is influenced by the material's silica and alumina content [37]. In other words, the higher the silica and alumina content, the greater the likelihood of an early and intense exothermic peak, which in turn will accelerate the geopolymer hardening process. These explanations could account for the extended setting time observed with the 30% GGBFS substitution.

### 1.3 Workability of geopolymer mortar

The workability of geopolymer mortar was assessed using flow table test as seen in Figure 4. The flow table test results for geopolymer mortar can be seen in Table 6 indicated a range of flow values from 83% to 158%, with the sample containing 100% GGBFS showing the lowest flow index and the sample with 100% FA demonstrating the highest flow index. The flow table test results were compared to the standards, where the standard minimum flow index ensures

the workability and ease of placement of the mortar into the mold. Results indicated that GGBFS replacements of 0%, 30%, and 50% met the requirement, except for 100% GGBFS replacement. Although the lowest flow index by the standard may be set at 105%, the workability criteria may depend on the particular construction application and the desired properties for the intended use.

From the results, it can be deduced that increasing the replacement of GGBFS reduces workability, which was consistent with prior studies [38], [39]. A study on class F FA and up to 30% addition of GGBFS, indicated a decrease in the slump and flow values with the incorporation of GGBFS, evidently in 30% addition decreased 10 cm slump [16]. Additionally, it was noted that increasing GGBFS content leads to more angular particles and fewer spherical particles compared to FA, which adversely affects flowability of geopolymer mixture [40].

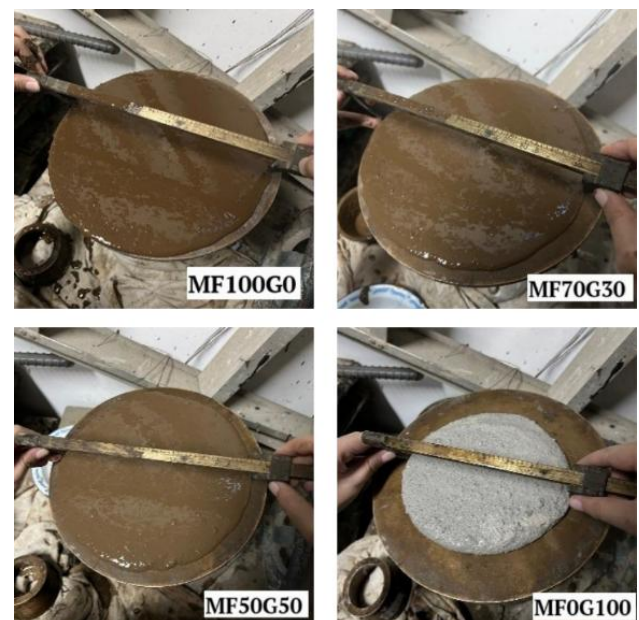


Figure 4 Flow table test of geopolymer mortar

Table 6. Flow test result of geopolymer mortar and minimum flow standard

Mix ID	Mix label	Flow diameter (mm)	Flow index (%)	Standards for minimum flow index
MF100G0	MF100G0M10A45B3R15Rm15	257.5	158	ASTM C1437: 105-115%.
MF70G30	MF70G30M10A45B3R15Rm15	248.75	149	IS 1727: 105 ± 5%.
MF50G50	MF50G50M10A45B3R15Rm15	237.5	138	EN 196: 110± 5%.
MF0G100	MF0G100M10A45B3R15Rm15	182.5	83	

### 1.4 Compressive strength of geopolymer paste and concrete

Geopolymer paste mixtures were tested as trials before making geopolymer concrete, the result as seen in Figure 5. The compressive strength of the paste was significantly enhanced by incorporating GGBFS into the mixture. This improvement was particularly notable at a 50% GGBFS replacement, where the paste achieved a compressive strength of 100.29 MPa at 28 days, significantly higher than

the strength of a paste containing only FA. The maximum paste compressive strength was achieved with 100% GGBFS, reaching 112.27 MPa at 28 days. The analysis revealed a notable trend: the incorporation of GGBFS into the concrete mix yielded a significant enhancement in compressive strength over the course of curing. The observed increase in compressive strength with the addition of GGBFS to geopolymer materials can be attributed to several underlying factors, such as enhanced reactivity, more

significant amount of soluble calcium oxide and denser matrix [41]. One significant contribution is the role of GGBFS in facilitating the formation of calcium-based reaction products, particularly C-(N)-A-S-H gels. These gels enhance the mechanical properties of the material by introducing an additional bonding phase within the geopolymer matrix. The abundance of available calcium ions in the GGBFS enables their reaction with alumina and silica present in the geopolymer mix. This reaction leads to the creation of C(A)SH gel, which acts as a reinforcing agent by enhancing the cohesion and overall density of the geopolymer matrix. This finding is supported by studies such as [16] and [42], which underscore the significant role of GGBFS in augmenting the compressive strength of geopolymer materials through the formation of calcium-based reaction products.

Compressive testing of geopolymer concrete was conducted at 1, 7, and 28 days of age, with results presented in Table 7. Based on the result, it is suggested that the FA-GGBFS-based geopolymer is a superior alternative to the FA-based geopolymer, as evidenced by the lowest compressive strength observed in the 100% FA mix (39.37 MPa). The highest concrete compressive strength was attained with 100% GGBFS, achieving 74.86 MPa at 28 days, albeit with lower workability. However, considering setting time, workability, and compressive strength collectively, the optimal ratio for geopolymer concrete was found to be a 50% replacement ratio, which achieved a compressive strength of 69.08 MPa.

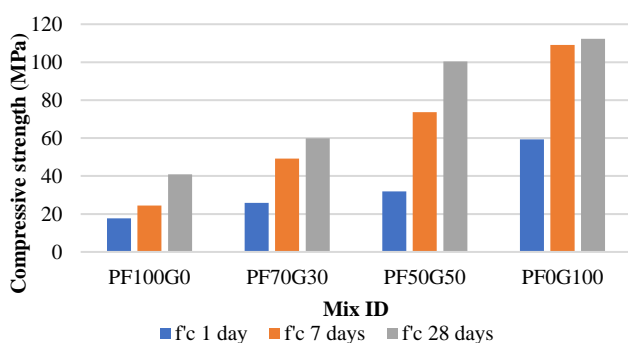


Figure 5. Compressive strength of geopolymer paste

Investigating deeper into the intricacies of strength development, the influence of GGBFS on early-age concrete properties emerged as particularly significant can be seen in Error! Reference source not found.. This trend was evident in mixes containing FA and GGBFS where notable strength gains were observed as early as day 1, especially when compared to the mixture containing only FA. Such enhanced early-age strength characteristics can have significant implications for construction projects, potentially allowing for quicker attainment of structural integrity and improved performance in the early stages of construction.

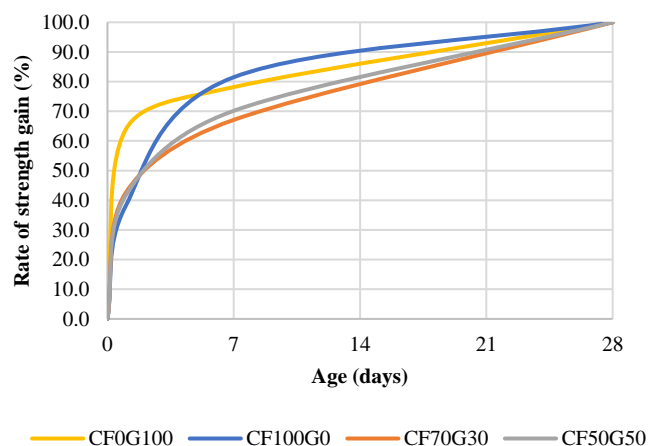


Figure 6. Rate of strength gain of geopolymer concrete

For comparison, various previous studies focusing on FA-GGBFS based geopolymer were examined alongside this study. The investigation has yielded noteworthy results, demonstrating that this study has attained the highest compressive strength when compared to those reported in the prior studies (based on studies provided in Table 8. The outcomes signify a substantial step forward in the development and understanding of FA-GGBFS based geopolymer.

Table 7. Compressive strength and rate of strength gain of geopolymer concrete

Mix ID	Mix label	Compressive strength (MPa)			Strength gain (%)	
		1 day	7 days	28 days	F’c 1/28	F’c 7/28
CF100G0	CF100G0M10A45B3R15RbRm15	14.94	32.09	39.37	37.9	81.5
CF70G30	CF70G30M10A45B3R15RbRm15	28.08	44.46	66.25	42.4	67.1
CF50G50	CF50G50M10A45B3R15RbRm15	28.65	48.47	69.08	41.5	70.2
CF0G100	CF0G100M10A45B3R15RbRm15	47.71	58.52	74.86	63.7	78.2

**Table 8.** Previous studies of FA-GGBFS based geopolymer

Authors	Precursor	Activator	R	M	A	Curing	Max $F'c$ 28 days (MPa)	Note
[16]	FA (F), GGBFS	SS, SH	1.5	14	0.35	Ambient	55(concrete);63 (mortar)	GGBFS 30%, concrete sample.
[43]	FA (F), GGBFS	SS, SH	2.5	8	0.4	Ambient	61.5	GGBFS fixed 30%, mortar sample.
[44]	FA (F), GGBFS	SS, SH	2.5	8	0.4	Ambient	56.63	GGBFS 30%, 150 mm cube concrete.
[13]	FA (F), GGBFS	SS, SH	2.5	12	0.48	Ambient	51.92	GGBFS fixed 50%, 2% nano alumina, concrete sample.
[14]	FA (F), GGBFS	SS, SH	2.5	12	0.48	Ambient	53.61	GGBFS fixed 50%, 0.3% Graphene Oxide, concrete sample.
[38]	FA (F), GGBFS	SS, SH	2.5	12	0.5	Ambient	63.37	concrete sample.
[45]	FA (F), GGBFS	SS, SH	2.5	8	0.45	Ambient	57.6	50% GGBFS, concrete sample.
[15]	FA (F), GGBFS	SS, SH, KOH (solid)				Ambient	30 -40	15-20% GGBFS, paste sample.
[46]	FA (C), GGBFS		1.5	10		Ambient	23.40	30% GGBFS, concrete sample.
[17]	FA (F), GGBFS	SS, SH	2.5	8	0.45	Ambient	45	30% GGBFS, concrete sample.
[47]	FA (F), GGBFS	SS, SH	1.5		0.3	Ambient	60	30% GGBFS, concrete sample.
[18]	FA (C), GGBFS	SS, SS + SH	1.5	4	0.4	Oven 60°C 24 h	56.43	100% GGBFS, paste sample.
[48]	FA (C), GGBFS	Na <sub>2</sub> CO <sub>3</sub>				Ambient	43.9	30% GGBFS, mortar sample.

#### 4. Conclusion

The addition of borax at 3% extended the setting time by 7-33 minutes compared to the mixture with 0% borax, suggesting borax's role as a retarder for FA-GGBFS-based geopolymer. Both initial and final setting times was prolonged with 30% replacement due to the highly reactive FA, while being accelerated with 50% and 100% GGBFS replacement. Geopolymer mortar flowability varied with GGBFS replacement, with flow values ranging from 83% to 158%; the 100% GGBFS sample exhibited the lowest flow index (83%), whereas the 100% FA sample showed the highest (158%). Incorporating GGBFS into the concrete mix notably enhanced compressive strength, particularly in early stages, with the highest achieved at 100% GGBFS (74.86 MPa), despite lower workability. Geopolymer paste with 50% GGBFS replacement reached 100.29 MPa compressive strength (28 days), while concrete with the same replacement attained 69.08 MPa. This study yielded the highest compressive strength reported to date (based on the previously referenced studies). The optimal ratio, balancing setting time, workability, and compressive strength, is attained with 50% GGBFS replacement, resulting in 40 minutes of initial setting time, a flow index of 138%, and compressive strength of 69.08 MPa.

#### Disclaimer

No conflicts of interest are declared by the authors.

#### Acknowledgments

We extend our sincere gratitude to PT Krakatau Semen Indonesia for providing the ground granulated blast furnace slag (GGBFS) used in this research. We also express our appreciation to CV Muncul Karya for supplying the

aggregates utilized in our experiments. Their contributions have been invaluable to the successful completion of this study.

#### References

- [1] R. M. Andrew, "Global CO<sub>2</sub> emissions from cement production," *Earth Syst Sci Data*, vol. 10, no. 1, pp. 195–217, Jan. 2018, doi: 10.5194/essd-10-195-2018.
- [2] F. Pacheco-Torgal, "Introduction to the environmental impact of construction and building materials," in *Eco-efficient Construction and Building Materials*, Elsevier, 2014, pp. 1–10. doi: 10.1533/9780857097729.1.
- [3] Md. F. S. Zawad, Md. A. Rahman, and S. N. Priyom, "Bio-Engineered Concrete: A Critical Review on The Next Generation of Durable Concrete," *Journal of the Civil Engineering Forum*, vol. 7, no. 3, p. 335, Aug. 2021, doi: 10.22146/jcef.65317.
- [4] K. C. Gomes, M. Carvalho, D. de P. Diniz, R. de C. C. Abrantes, M. A. Branco, and P. R. O. de Carvalho Junior, "Carbon emissions associated with two types of foundations: CP-II Portland cement-based composite vs. geopolymer concrete," *Matéria (Rio de Janeiro)*, vol. 24, no. 4, 2019, doi: 10.1590/s1517-707620190004.0850.
- [5] A. N. Beskopylny *et al.*, "Developing Environmentally Sustainable and Cost-Effective Geopolymer Concrete with Improved Characteristics," *Sustainability*, vol. 13, no. 24, p. 13607, Dec. 2021, doi: 10.3390/su132413607.
- [6] B. C. McLellan, R. P. Williams, J. Lay, A. van Riessen, and G. D. Corder, "Costs and carbon emissions for

- geopolymer pastes in comparison to ordinary portland cement,” *J Clean Prod*, vol. 19, no. 9–10, pp. 1080–1090, Jun. 2011, doi: 10.1016/j.jclepro.2011.02.010.
- [7] T. Błaszczyszński and M. Król, “Usage of Green Concrete Technology in Civil Engineering,” *Procedia Eng*, vol. 122, pp. 296–301, 2015, doi: 10.1016/j.proeng.2015.10.039.
- [8] K. K. D. Sungkono, I. Satyarno, H. Priyosulistyo, and I. Perdana, “Corrosion Resistance of High Calcium Fly Ash Based Reinforced Geopolymer Concrete in Marine Environment,” *Civil Engineering and Architecture*, vol. 11, no. 5A, pp. 3175–3189, Sep. 2023, doi: 10.13189/cea.2023.110827.
- [9] I. Garcia Lodeiro, N. Cristelo, A. Palomo, and A. Fernández-Jiménez, “Use of industrial by-products as alkaline cement activators,” *Constr Build Mater*, vol. 253, p. 119000, Aug. 2020, doi: 10.1016/j.conbuildmat.2020.119000.
- [10] M. Olivia, L. M. Tambunan, and E. Saputra, “Properties of Palm Oil Fuel Ash (POFA) Geopolymer Mortar Cured at Ambient Temperature,” *MATEC Web of Conferences*, vol. 97, p. 01006, Feb. 2017, doi: 10.1051/mateconf/20179701006.
- [11] L. S. Wong, “Durability Performance of Geopolymer Concrete: A Review,” *Polymers (Basel)*, vol. 14, no. 5, p. 868, Feb. 2022, doi: 10.3390/polym14050868.
- [12] S. Parathi, P. Nagarajan, and S. A. Pallikkara, “Ecofriendly geopolymer concrete: a comprehensive review,” *Clean Technol Environ Policy*, vol. 23, no. 6, pp. 1701–1713, Aug. 2021, doi: 10.1007/s10098-021-02085-0.
- [13] N. A. K. Reddy and K. Ramujee, “Comparative study on mechanical properties of fly ash-GGBFS based geopolymer concrete and OPC concrete using nano-alumina,” *Mater Today Proc*, vol. 60, pp. 399–404, Jan. 2022, doi: 10.1016/j.matpr.2022.01.260.
- [14] S. S. S and R. Kolli, “Experimental investigation on mechanical properties of fly ash-GGBFS based GO-geopolymer concrete using mineral sand (Quartz-Feldspar) as fine aggregate,” *Mater Today Proc*, vol. 60, pp. 40–45, Jan. 2022, doi: 10.1016/j.matpr.2021.11.325.
- [15] S. Y. Oderji, B. Chen, M. R. Ahmad, and S. F. A. Shah, “Fresh and hardened properties of one-part fly ash-based geopolymer binders cured at room temperature: Effect of slag and alkali activators,” *J Clean Prod*, vol. 225, pp. 1–10, Jul. 2019, doi: 10.1016/j.jclepro.2019.03.290.
- [16] P. Nath and P. K. Sarker, “Effect of GGBFS on setting, workability and early strength properties of fly ash geopolymer concrete cured in ambient condition,” *Constr Build Mater*, vol. 66, pp. 163–171, Sep. 2014, doi: 10.1016/j.conbuildmat.2014.05.080.
- [17] S. Nagajothi and S. Elavenil, “Effect of GGBS Addition on Reactivity and Microstructure Properties of Ambient Cured Fly Ash Based Geopolymer Concrete,” *Silicon*, vol. 13, pp. 507–516, 2021, doi: 10.1007/s12633-020-00470-w/Published.
- [18] S. Sasui, G. Kim, J. Nam, T. Koyama, and S. Chansomsak, “Strength and Microstructure of Class-C Fly Ash and GGBS Blend Geopolymer Activated in NaOH & NaOH + Na<sub>2</sub>SiO<sub>3</sub>,” *Materials*, vol. 13, no. 1, p. 59, Dec. 2019, doi: 10.3390/ma13010059.
- [19] X. Chen and P. Mondal, “Sucrose retards the reaction of non-calcium geopolymers: An implication for developing kinetics-controlling admixtures,” *Journal of the American Ceramic Society*, vol. 104, no. 6, pp. 2894–2907, Jun. 2021, doi: 10.1111/jace.17706.
- [20] B. Nematollahi and J. Sanjayan, “Effect of different superplasticizers and activator combinations on workability and strength of fly ash based geopolymer,” *Mater Des*, vol. 57, pp. 667–672, May 2014, doi: 10.1016/j.matdes.2014.01.064.
- [21] A. Antoni, A. A. T. Purwantoro, W. S. P. D. Suyanto, and D. Hardjito, “Fresh and Hardened Properties of High Calcium Fly Ash-Based Geopolymer Matrix with High Dosage of Borax,” *Iranian Journal of Science and Technology - Transactions of Civil Engineering*, vol. 44, pp. 535–543, Oct. 2020, doi: 10.1007/s40996-019-00330-7.
- [22] R. Cornelis, H. Priyosulistyo, and I. Satyarno, “Workability and Strength Properties of Class C Fly Ash-Based Geopolymer Mortar,” in *Sustainable Civil Engineering Structures and Construction Materials*, 2018. doi: 10.1051/mateconf/20192.
- [23] M. Putri, I. Satyarno, and D. Sulistyono, “Pengaruh Penambahan Borax terhadap Setting Time Pasta Geopolymer Berbahan Dasar Fly Ash dan Ground Granulated Blast Furnace Slag,” in *Simposium Nasional Teknologi Infrastruktur*, Yogyakarta, 2024.

- [24] H. Ma *et al.*, “Preparation and Reaction Mechanism Characterization of Alkali-activated Coal Gangue–Slag Materials,” *Materials*, vol. 12, no. 14, p. 2250, Jul. 2019, doi: 10.3390/ma12142250.
- [25] R. M. Waqas, F. Butt, X. Zhu, T. Jiang, and R. F. Tufail, “A Comprehensive Study on the Factors Affecting the Workability and Mechanical Properties of Ambient Cured Fly Ash and Slag Based Geopolymer Concrete,” *Applied Sciences*, vol. 11, no. 18, p. 8722, Sep. 2021, doi: 10.3390/app11188722.
- [26] T. W. Cheng and J. P. Chiu, “Fire-resistant geopolymer produced by granulated blast furnace slag,” *Miner Eng*, vol. 16, no. 3, pp. 205–210, Mar. 2003, doi: 10.1016/S0892-6875(03)00008-6.
- [27] P. Pavithra, M. Srinivasula Reddy, P. Dinakar, B. Hanumantha Rao, B. K. Satpathy, and A. N. Mohanty, “Effect of the  $\text{Na}_2\text{SiO}_3/\text{NaOH}$  Ratio and  $\text{NaOH}$  Molarity on the Synthesis of Fly Ash-Based Geopolymer Mortar,” in *Geo-Chicago 2016*, Reston, VA: American Society of Civil Engineers, Aug. 2016, pp. 336–344. doi: 10.1061/9780784480151.034.
- [28] I. Satyarno, A. P. Solehudin, C. Meyarto, D. Hadiyatmoko, P. Muhammad, and R. Afnan, “Practical Method for Mix Design of Cement-based Grout,” *Procedia Eng*, vol. 95, pp. 356–365, Jan. 2014, doi: 10.1016/J.PROENG.2014.12.194.
- [29] H. Liu, J. G. Sanjayan, and Y. Bu, “The application of sodium hydroxide and anhydrous borax as composite activator of class F fly ash for extending setting time,” *Fuel*, vol. 206, pp. 534–540, Oct. 2017, doi: 10.1016/j.fuel.2017.06.049.
- [30] S. E. Thomas, A. Muhsin Lebba, S. Sreeja, and K. P. Ramaswamy, “Effect of borax in slag-fly ash-based alkali activated paste,” *IOP Conf Ser Earth Environ Sci*, vol. 1237, no. 1, p. 012006, Sep. 2023, doi: 10.1088/1755-1315/1237/1/012006.
- [31] P. Li, D. Chen, Z. Jia, Y. Li, S. Li, and B. Yu, “Effects of Borax, Sucrose, and Citric Acid on the Setting Time and Mechanical Properties of Alkali-Activated Slag,” *Materials*, vol. 16, no. 8, p. 3010, Apr. 2023, doi: 10.3390/ma16083010.
- [32] T. Pahlawan, J. Tarigan, J. J. Ekaputri, and A. Nasution, “Effect of Borax on Very High Calcium Geopolymer Concrete,” *Int J Adv Sci Eng Inf Technol*, vol. 13, no. 4, pp. 1387–1392, Aug. 2023, doi: 10.18517/ijaseit.13.4.18291.
- [33] J. Yang and C. Qian, “Effect of borax on hydration and hardening properties of magnesium and potassium phosphate cement pastes,” *Journal of Wuhan University of Technology-Mater. Sci. Ed.*, vol. 25, no. 4, pp. 613–618, Aug. 2010, doi: 10.1007/s11595-010-0055-6.
- [34] P. Nuaklong, K. Janprasit, and P. Jongvivatsakul, “Enhancement of strengths of high-calcium fly ash geopolymer containing borax with rice husk ash,” *Journal of Building Engineering*, vol. 40, Aug. 2021, doi: 10.1016/j.jobe.2021.102762.
- [35] Y. Ling, K. Wang, W. Li, G. Shi, and P. Lu, “Effect of slag on the mechanical properties and bond strength of fly ash-based engineered geopolymer composites,” *Compos B Eng*, vol. 164, pp. 747–757, May 2019, doi: 10.1016/j.compositesb.2019.01.092.
- [36] M. N. S. Hadi, N. A. Farhan, and M. N. Sheikh, “Design of geopolymer concrete with GGBFS at ambient curing condition using Taguchi method,” *Constr Build Mater*, vol. 140, pp. 424–431, Jun. 2017, doi: 10.1016/j.conbuildmat.2017.02.131.
- [37] P. Chindaprasirt, P. De Silva, K. Sagoe-Crentsil, and S. Hanjitsuwan, “Effect of  $\text{SiO}_2$  and  $\text{Al}_2\text{O}_3$  on the setting and hardening of high calcium fly ash-based geopolymer systems,” *J Mater Sci*, vol. 47, no. 12, pp. 4876–4883, Jun. 2012, doi: 10.1007/s10853-012-6353-y.
- [38] Q. Zhong, X. Tian, G. Xie, X. Luo, and H. Peng, “Investigation of Setting Time and Microstructural and Mechanical Properties of MK/GGBFS-Blended Geopolymer Pastes,” *Materials*, vol. 15, no. 23, p. 8431, Nov. 2022, doi: 10.3390/ma15238431.
- [39] B. Kanagaraj, A. N. U. J. Alengaram, S. Raj R, P. B. and K. Tattukolla, “Performance evaluation on engineering properties and sustainability analysis of high strength geopolymer concrete,” *Journal of Building Engineering*, vol. 60, Nov. 2022, doi: 10.1016/j.jobe.2022.105147.
- [40] P. S. Deb, P. Nath, and P. K. Sarker, “Properties Of Fly Ash And Slag Blended Geopolymer Concrete Cured At Ambient Temperature,” in *Proceedings of the New Developments in Structural Engineering and Construction*, Singapore: Research Publishing Services, 2013, pp. 571–576. doi: 10.3850/978-981-07-5354-2\_M-55-433.
- [41] M. H. Al-Majidi, A. Lampropoulos, A. Cundy, and S. Meikle, “Development of geopolymer mortar under ambient temperature for in situ applications,” *Constr*

- Build Mater*, vol. 120, pp. 198–211, Sep. 2016, doi: 10.1016/j.conbuildmat.2016.05.085.
- [42] W. Teo, K. Shirai, J. H. Lim, L. B. Jack, and E. Nikbakht, “Experimental Investigation on Ambient-Cured One-Part Alkali-Activated Binders Using Combined High-Calcium Fly Ash (HCFA) and Ground Granulated Blast Furnace Slag (GGBS),” *Materials*, vol. 15, no. 4, Feb. 2022, doi: 10.3390/ma15041612.
- [43] Z. Zhang, J. L. Provis, A. Reid, and H. Wang, “Mechanical, thermal insulation, thermal resistance and acoustic absorption properties of geopolymer foam concrete,” *Cem Concr Compos*, vol. 62, pp. 97–105, Sep. 2015, doi: 10.1016/j.cemconcomp.2015.03.013.
- [44] R. R. Bellum, “Influence of steel and PP fibers on mechanical and microstructural properties of fly ash-GGBFS based geopolymer composites,” *Ceram Int*, vol. 48, no. 5, pp. 6808–6818, Mar. 2022, doi: 10.1016/j.ceramint.2021.11.232.
- [45] R. R. Bellum, K. Muniraj, and S. R. C. Madduru, “Characteristic Evaluation of Geopolymer Concrete for the Development of Road Network: Sustainable Infrastructure,” *Innovative Infrastructure Solutions*, vol. 5, no. 3, p. 91, Dec. 2020, doi: 10.1007/s41062-020-00344-5.
- [46] R. R. Bellum, K. Muniraj, and S. R. C. Madduru, “Influence of slag on mechanical and durability properties of fly ash-based geopolymer concrete,” *Journal of the Korean Ceramic Society*, vol. 57, no. 5, pp. 530–545, Sep. 2020, doi: 10.1007/s43207-020-00056-7.
- [47] A. Wardhono, D. W. Law, and A. Strano, “The Strength of Alkali-activated Slag/fly Ash Mortar Blends at Ambient Temperature,” *Procedia Eng*, vol. 125, pp. 650–656, 2015, doi: 10.1016/j.proeng.2015.11.095.
- [48] B. Gopalakrishna and P. Dinakar, “Mix design development of fly ash-GGBS based recycled aggregate geopolymer concrete,” *Journal of Building Engineering*, vol. 63, Jan. 2023, doi: 10.1016/j.job.2022.105551.
- [49] A. Brykov and M. Voronkov, “Dry Mix Slag—High-Calcium Fly Ash Binder. Part One: Hydration and Mechanical Properties,” *Materials Sciences and Applications*, vol. 14, no. 03, pp. 240–254, 2023, doi: 10.4236/msa.2023.143014.